Quaternary Research (2023), 1–17
doi:10.1017/qua.2022.62

Research Article

Discovering fire events in the HAS1 settlement on the Dhofar coast (Oman) by a multi-methodological study of mollusk shells

Gaia Crippa[a]*, Silvia Lischi[b], Andrea Chiari[a], Monica Dapiaggi[a] and Mauro Cremaschi[a]

[a]Università degli Studi di Milano, Dipartimento di Scienze della Terra 'A. Desio', via Mangiagalli 34, Milano, 20133, Italy and [b]Università degli Studi di Pisa, Dipartimento di Civiltà e Forme del Sapere, Via Pasquale Paoli 15, Pisa, 56100, Italy

Abstract

Mollusk shells from archeological deposits are often exposed to high temperatures through human-caused or natural heating events. While heat exposure affects reliability of mollusk shells for environmental reconstructions based on geochemistry, it can provide a valuable source of information on past human behaviors and human–environment interactions. We analyzed burned and not-burned bivalve and gastropod specimens collected within two megalithic circular structures in the HAS1 settlement in Oman (Late Iron Age and Classical Period). Through a multi-methodological approach, we investigated shell microstructure using scanning electron microscopy (SEM), shell mineralogy using X-ray diffraction (XRD), and shell stable-isotopic composition ($\delta^{18}O$, $\delta^{13}C$) using isotope-ratio mass spectrometry (IRMS) to infer the temperatures these specimens were exposed to and to reconstruct the processes responsible for heating the shells. Thermal response of aragonite and calcite shells having different microstructures were also determined. We found that mollusk shells at this site were exposed to three temperature ranges: a) no exposure or <300°C, b) between 250°C and 500°C, and c) ≥500°C. The heat source was likely a fire which engulfed the entire settlement, which is also supported by evidence of carbonized wooden poles found in situ inside the circular structures.

Keywords: Mollusk shells, Microstructure, Stable isotopes, Mineralogy, Fire, Archaeology, Oman

(Received 11 March 2022; accepted 20 October 2022)

INTRODUCTION

Mollusk shells are excellent archives of proxies that provide a large amount of useful information for unraveling Earth's deep and recent past (e.g., Ivany and Runnegar, 2010; Schöne and Surge, 2012). In the recent past, shells from archaeological sites have shown a significant and growing potential for reconstructing paleoenvironments and human–environment interactions (e.g., Andrus, 2011; Milano et al., 2016; Campbell, 2017). Faunal resources of adjacent aquatic environments have been often exploited by coastal human populations (Richards et al., 2005; Müller et al., 2017) who gathered shells for many different purposes (e.g., fish bait, dye production, material for adornments or tools), but mainly for food (Campbell, 2017). Indeed, mollusks or other faunal remains were often accumulated near settlements to form shell middens. If the study of the composition and internal structure of these shell middens can provide valuable information about human dispersal, settlement patterns, subsistence strategies, associated dietary habits, or fishing and foraging seasonality (Müller et al., 2017), other important and useful information can be gained from high-resolution analyses of mollusk shell biominerals.

Mollusk shells are considered one of the best archives of proxies to document past oceanic conditions because they record physical and chemical conditions of the environment in which they lived, generally with no vital effect (e.g., Epstein et al., 1953; O'Neil et al., 1969; Lécuyer et al., 2004; Schöne, 2008), building carbonate shells episodically rather than continuously (e.g., Ivany and Runnegar, 2010; Schöne and Surge, 2012). The discipline analyzing the periodic physical and chemical variations recorded in the hard parts of organisms and the temporal context in which they are produced is called sclerochronology (e.g., Jones, 1983; Gröcke and Gillikin, 2008; Oschmann, 2009; Schöne and Gillikin, 2013). Powerfully applied to geological and modern settings for seasonal (paleo)environmental reconstructions, sclerochronology has been recently applied also to archeological sites (e.g., Mannino et al., 2003; Andrus, 2011; Lindauer et al., 2017; Butler et al., 2019), through the analysis of the shell stable-isotope compositions ($\delta^{18}O$, $\delta^{13}C$). Indeed, the $\delta^{18}O$ recorded by the shell provides information about the season of mollusk collection contributing to the knowledge of ancient subsistence practices and site occupation (e.g., Shackleton, 1973; Mannino et al., 2003, 2007, 2011; Burchell et al., 2013; Eerkens et al., 2013; Prendergast et al., 2016). From a paleoenvironmental point of view, shell $\delta^{18}O$ is traditionally used as paleothermometer (e.g., Urey, 1947; Epstein et al., 1953; Brand et al., 2011, 2019 and reference therein; Schöne and Surge, 2012), but it can provide also information about salinity fluctuations (e.g., Ingram et al., 1996). The $\delta^{13}C$, although more complex to interpret due to variable and

*Corresponding author email address: <gaia.crippa@unimi.it>

Cite this article: Crippa G, Lischi S, Chiari A, Dapiaggi M, Cremaschi M (2023). Discovering fire events in the HAS1 settlement on the Dhofar coast (Oman) by a multi-methodological study of mollusk shells. *Quaternary Research* 1–17. https://doi.org/10.1017/qua.2022.62

unpredictable vital effects, can be a useful indicator of environmental conditions, such as primary production or salinity changes (e.g., Gillikin et al., 2006; McConnaughey and Gillikin, 2008; Crippa et al., 2016a).

However, mollusks in archeological sites may have undergone high temperature exposure, experiencing processes like cooking by boiling or roasting or uncontrolled fire which can modify their shell mineralogy, microstructure and isotope composition (e.g., Andrus and Crowe, 2002; Milano et al., 2016, 2018); this may lead to erroneous reconstructions, as the shell isotope signature no longer reflects the ambient environmental conditions at the time of biomineral deposition. According to Larsen (2015), archeologists expect heated shells to look burned or badly preserved, so they often select fossil specimens for paleoenvironmental reconstructions based on their external appearance without performing further tests to check their preservation. However, altered shells may not be easily identifiable at first sight. As observed by Milano et al. (2016, 2018), boiling or roasting at moderate temperatures and indirect fire exposure may not necessarily alter the shell surface, whereas roasting at high temperatures causes a drastic surface blackening.

Given the abundance of heated shells in archeological sites, it is important to understand the effects of heating on the physicochemical structure of mollusk shells. In the last few years, many studies (e.g., Larsen, 2015; Li et al., 2015; Milano et al., 2016, 2018; Müller et al., 2017; Lindauer et al., 2018; Milano and Nehrke, 2018; Aldeias et al., 2019) simulated cooking methods by boiling and/or roasting modern mollusk shells at different temperatures and for different time intervals to observe the effects of these processes on the mineralogy, microstructure, stable isotope composition, and radiocarbon dating, focusing mainly on aragonite specimens.

Based on these previous findings, we selected both burned and not-burned bivalve and gastropod shells belonging to six originally calcite- or aragonite-shelled species having different microstructures (crossed-lamellar, nacre, and foliated). The recently discovered HAS1 site in Oman (Fig. 1) is of fundamental importance for understanding the indigenous population of the area and their habits. Until now, the presence of a local population had been proposed (Morandi Bonacossi, 2004; Newton and Zarins, 2019), but never systematically studied. Since its discovery in 2016, this settlement has been investigated to understand its characteristics, chronology, and relations with the nearby South Arabian city of Sumhuram (Lischi, 2019a, b, 2021).

The aim of our research is to infer the temperatures these archeological mollusk shells were exposed to using a consolidated, multi-methodological approach to reconstruct the processes responsible for heating the shells, and to better comprehend past human behaviors and the events that took place in the HAS1 settlement during the Iron Age and the Classical Period.

MATERIAL

Sixteen specimens of bivalves and gastropods were analyzed (Fig. 2; Table 1). Specimens were collected from the HAS1 settlement, which is located on the northern plateau of the Inqitat promontory in the Khor Rhori Archeological Park about 40 km east of Salalah, Dhofar region, southern Oman (17°01'45.2"N, 54°26'32.4"E; Fig. 1A, B). The settlement is made up of circular megalithic structures consisting of a stone basement made by a sandwich wall, which is filled with soil mixed with rocks of different sizes (Fig. 1C). The upper part of the structure is not preserved but was probably made up of perishable material supported by wooden poles. Traces of the poles and the roof were found carbonized in situ during excavation activities.

The mollusk specimens analyzed herein come from two stratigraphic units within two circular structures (stratigraphic unit US30 in circular structure B5, and stratigraphic unit US54 in circular structure B9; Fig. 1C). Stratigraphic unit US30 is the lowest layer found in circular structure B5. Most of the materials in this unit has been dated to the first century BC to the early second century AD, but some are probably related to previous occupation of the site that has been dated to 2195 ± 45 yr BP (Lischi, 2019a). Unit US30 is composed of large fragments of charcoal mixed mainly with medium and small stones with rare big stones. Wooden poles that are completely carbonized occur above and below the stones, and almost complete potteries were found within this layer and on the floor of the structure. These characteristics allowed us to recognize this as the layer representing collapse of the circular structure. Stratigraphic unit US54 is a layer

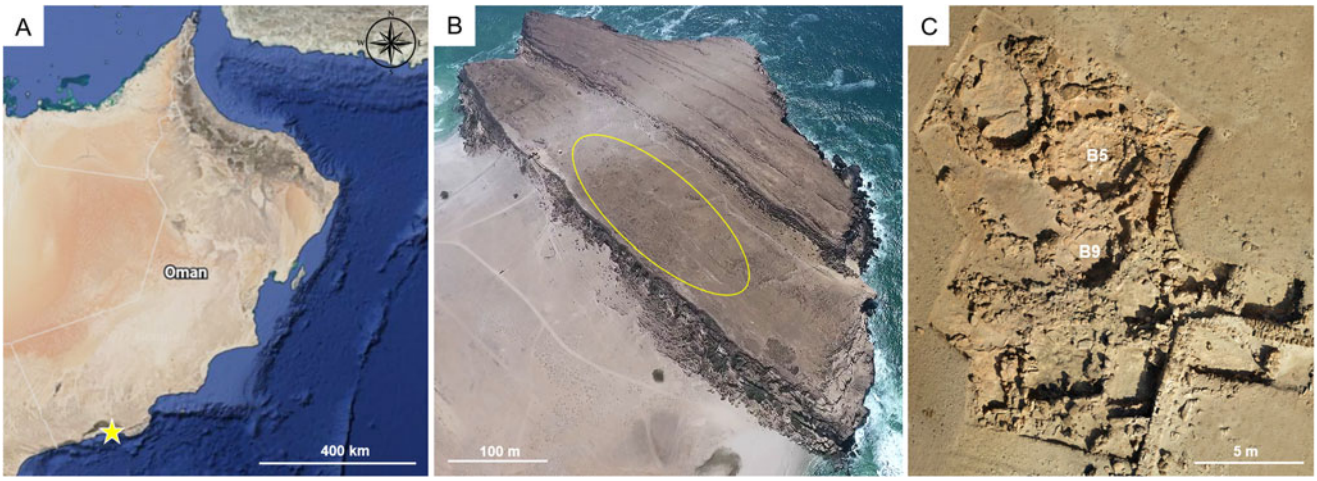

Figure 1. Photographs of Oman showing: (A) location of the HAS1 settlement in the Dhofar region (yellow star), lines represent state territorial borders; source: GoogleEarth; (B) the northern plateau of the Inqitat promontory where the HAS1 settlement is situated (inside yellow oval), source: drone reconnaissance; (C) HAS1 settlement showing position of the circular structures studied (B5, B9), source: drone reconnaissance.

https://doi.org/10.1017/qua.2022.62 Published online by Cambridge University Press

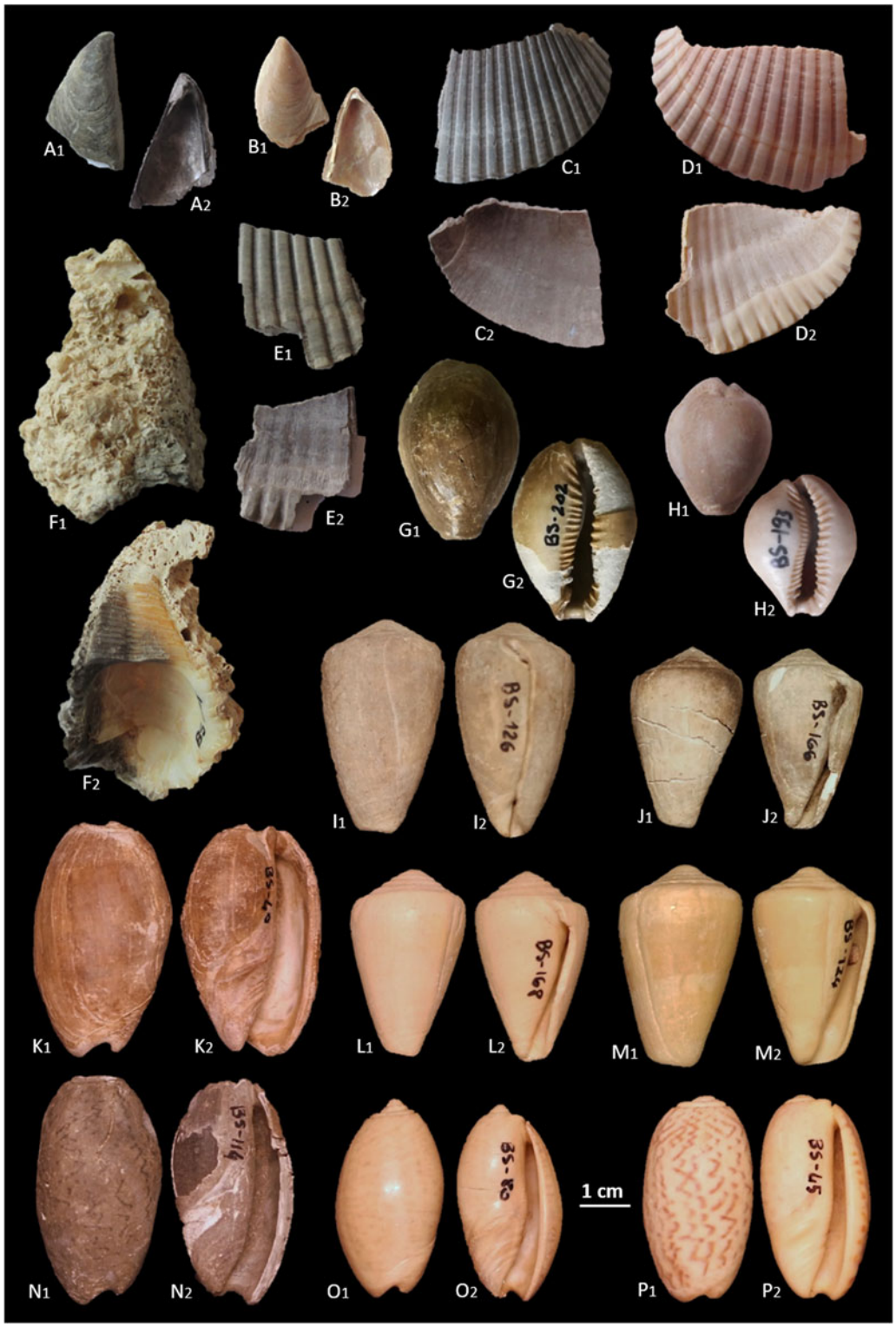

Figure 2. Burned and not-burned mollusk specimens analyzed in this study with two views shown for each specimen: external (1) or internal (2) for bivalves, abapertural (1) or apertural (2) for gastropods; field numbers given for each specimen. All specimens reposited in Dipartimento di Scienze della Terra 'A. Desio' of the University of Milan; see text for repository numbers. (A1, A2; B1, B2) *Perna perna* (A: BS-304; B: BS-303); (C1, C2; D1, D2; E1, E2) *Anadara uropigimelana* (C: BS-301; D: BS-300; E: BS-302); (F1, F2) *Saccostrea cucullata* (BS-261); (G1, G2; H1, H2) *Naria* sp. (G: BS-202; H: BS-193); (I1, I2; J1, J2; L1, L2; M1, M2) *Conus* sp. (I: BS-126; J: BS-166; L: BS-168; M: BS-124); (K1, K2; N1, N2; O1, O2; P1, P2) *Oliva bulbosa* (K: BS-40; N: BS-114; O: BS-80; P: BS-45).

found inside the circular structure B9, where in situ carbonized wooden beams and many fire traces occur; this layer is nearly coeval with the US30 layer.

The settlement is dated to the Meghalayan (Upper Holocene) and based on archeological findings, was inhabited from at least the fourth century BC until the first to second century AD

https://doi.org/10.1017/qua.2022.62 Published online by Cambridge University Press

Table 1. Species analyzed with corresponding field ID number and Dipartimento di Scienze della Terra 'A. Desio' of the University of Milan (MPUM) repository number; color, microstructure, mineralogy, stable isotope composition, and hypothesized exposure temperature for each specimen.

						Isotope composition		Supposed exposure temperature
	Species	ID number	Color	Microstructure	Mineralogy	$\delta^{18}O$ (‰)	$\delta^{13}C$ (‰)	
Gastropoda	*Oliva bulbosa*	BS-45 (MPUM 12753)	Beige/light brown with color ornamentation	Crossed lamellae	100% aragonite	+0.23	+1.47	<300°C
		BS-80 (MPUM 12754)	Beige/light brown	Crossed lamellae	94% aragonite 6% calcite	+0.17	+0.38	250–500°C
		BS-40 (MPUM 12755)	Dark brown	Crossed lamellae and few recrystallized prisms	83% aragonite 17% calcite	−0.06	+1.33	250–500°C
		BS-114 (MPUM 12756)	Dark gray	Recrystallized prisms	100% calcite	−0.27	+0.53	≥500°C
	Conus sp.	BS-124 (MPUM 12757)	Beige/light brown	Crossed lamellae	100% aragonite	+0.27	+0.42	<300°C
		BS-168 (MPUM 12758)	Beige/light brown	Crossed lamellae	100% aragonite	+0.40	+1.34	<300°C
		BS-126 (MPUM 12759)	Gray	Crossed lamellae	100% aragonite	+0.39	+2.50	<300°C
		BS-166 (MPUM 12760)	Gray/brown	Recrystallized prisms and relict of crossed lamellae	5% aragonite 95% calcite	−0.15	+1.27	250–500°C
	Naria sp.	BS-193 (MPUM 12761)	Light brown	Crossed lamellae	98% aragonite 2% calcite	+0.24	+2.62	250–500°C
		BS-202 (MPUM 12762)	Dark brown/gray	Crossed lamellae and few recrystallized prisms	84% aragonite 16% calcite	+0.86	+2.31	250–500°C
Bivalvia	*Anadara uropigimelana*	BS-300 (MPUM 12763)	Beige/light brown	Crossed lamellae	100% aragonite	−0.55	−0.16	<300°C
		BS-301 (MPUM 12764)	Light gray	Crossed lamellae and few recrystallized prisms	85% aragonite 15% calcite	−0.33	−0.59	250–500°C
		BS-302 (MPUM 12765)	Light gray	Recrystallized prisms and relict crossed lamellae	13% aragonite 87% calcite	−0.85	−0.86	250–500°C
	Perna perna	BS-303 (MPUM 12766)	Beige/light brown	Nacre	100% aragonite	+0.25	+1.27	<300°C
		BS-304 (MPUM 12767)	Dark gray	Recrystallized prisms and relict nacre	100% calcite	−1.65	−1.05	≥500°C
	Saccostrea cucullata	BS-261W (MPUM 12768)	Beige	Foliated	100% calcite	−0.89	+0.82	<500°C
		BS-261B (MPUM 12768)	Dark gray	Foliated with rare recrystallized prisms	100% calcite	−0.31	+0.63	<500°C

(Late Iron Age and Classical Period; Lischi, 2018). The entire settlement was probably destroyed by a fire, and later, the structures were obliterated by wind accumulation. Above the abandonment phase of the area, traces of Islamic use of the area have been found. Numerous mollusk shells have been found both inside the megalithic circular structures and in a rubbish dump near the settlement. However, burned shells in the middens are nearly absent, whereas they are common in the circular structures (Table 2). For this reason, the burned shells we analyzed were selected from these two nearly coeval layers (US30 and US54), allowing us to investigate the events that occurred during the last phase of the settlement.

All the specimens we analyzed are housed in the collections of the Dipartimento di Scienze della Terra 'A. Desio' of the University of Milan, and registered with reference numbers consisting of a prefix MPUM followed by a five-digit number. Field numbers given in parentheses after the reference numbers. Gastropod specimens were identified as: *Oliva bulbosa* (Röding, 1798) [MPUM 12755 (BS-40), MPUM 12753 (BS-45), MPUM 12754 (BS-80), MPUM 12756 (BS-114)], *Conus* sp. [MPUM 12757 (BS-124), MPUM 12759 (BS-126), MPUM 12760 (BS-166), MPUM 12758 (BS-168)] and *Naria* sp. [MPUM 12761 (BS-193), MPUM 12762 (BS-202)].

Bivalves were identified as *Perna perna* (Linnaeus, 1858) [left valve, MPUM 12766 (BS-303), right valve MPUM 12767 (BS-304)], *Anadara uropigimelana* (Bory de Saint-Vincent, 1827) [fragments; MPUM 12763 (BS-300), MPUM 12764 (BS-301), MPUM 12765 (BS-302)], and *Saccostrea cucullata* (Born, 1778) [left valve; MPUM 12768 (BS-261B, dark colored area; BS-261W, light colored area)].

O. bulbosa, Conus sp., *Naria* sp. and *A. uropigimelana* have mainly aragonite crossed-lamellar shells (Kobayashi and Kamiya, 1968; Taylor et al., 1969; Carter, 1990; Tursch and Machbaete, 1995; Rodriguez-Navarro et al., 2012); *P. perna* has an aragonite nacreous shell (Taylor et al., 1969; Carter, 1990), whereas the left valve of *S. cucullata* is calcite crossed-foliated (Taylor et al., 1969; Carter, 1990). The choice of these species was made due to their aragonite composition. Aragonite is a metastable form of calcium carbonate, and when a shell undergoes diagenetic alteration or heating, the aragonite in the shell is commonly replaced by calcite (e.g., Milano et al., 2016; Casella et al., 2017); thus, changes due to increased temperatures should be easily observable at a microscopic level. For each species, at least two specimens were selected: one showing a dark color (black, gray, brown; i.e., inferred to have been exposed to high temperatures), and one showing a light color (light brown or beige; i.e., inferred to not have been exposed to high temperatures). The specimen of *S. cucullata* was chosen for its uniqueness: in the same shell, both a dark and a light area were present.

Table 2. Number of burned shells found in stratigraphic unit US30 in circular structure B5, and stratigraphic unit US54 in circular structure B9, divided by species. Bold numbers = number of burned shells; numbers in brackets = total number of specimens for each species found in the two structures; * indicates taxa used for food consumption; other taxa were used for other purposes, such as ornaments (Carenti and Wilkens 2008; Lischi, 2018).

Phylum Mollusca	US30, B5	US54, B9
Class Bivalvia		
Anadara uropigimelana (Bory de Saint-Vincent, 1827)*	**3 + fragments** (9)	
Perna perna (Linnaeus, 1758)*	**2** (5)	
Ostrea sp.*	**2** (3)	
Saccostrea cucullata (Born, 1778)*	**2** (2)	
Class Gastropoda		
Oliva bulbosa (Röding, 1798)	**30** (114)	**6** (46)
Naria ocellata (Linnaeus, 1758)	**1** (5)	
Naria turdus (Lamarck, 1810)	**1** (3)	
Naria sp.	**4** (12)	**2** (8)
Conus cf. *C. terebra* Born, 1778		**1** (1)
Conus namocanus Hwass in Bruguière, 1792	**3** (4)	**1** (2)
Conus sp.	**11** (51)	**1** (25)
Purpura panama (Röding, 1798)	**2** (9)	
Babylonia spirata (Linnaeus, 1758)*	**1** (4)	
Bullia semiplicata Gray in Griffith & Pidgeon, 1833	**3** (16)	
Bullia othaeitensis (Bruguière, 1789)	**1** (1)	
Ancilla castanea (G.B. Sowerby I, 1830)	**1** (2)	
Mitridae indet.	**1** (2)	
TOTAL	**68** (242)	**11** (82)

METHODS

Mollusk specimens were first cleaned from the sediment using a brush to gently remove the soft sediment, then washed with demineralized water and air-dried. They were then visually inspected focusing on color and fragility (prone to breakage).

To characterize the microstructure, shell sections were investigated using a JSM-IT500 (JEOL Spa, Italy) scanning electron microscope (SEM) at the Dipartimento di Scienze della Terra of the University of Milan, Italy. For sample preparation, we followed the procedure proposed by Crippa et al. (2016b) for fossil brachiopod shells. Specimens were cut in half longitudinally along the major axis except for the specimen of *S. cucullata*, which was cut transversally. One-half of each shell was then embedded in a transparent, bicomponent epoxy resin to form a small block. Sections of the *S. cucullata* valve were also observed without resin embedding. Each block/section was ground smooth using silicon carbide (SiC) powder of two different granulometries and etched with 5% HCl for 10 seconds to reveal the detail of the microstructure. After washing with demineralized water and drying, each block/section was coated with gold and observed using a SEM. More than 200 photos were taken using a SEM; each shell was carefully analyzed along the entire sectioned surface, i.e., from the outer to the inner shell layer and from the dorsal to the ventral region in bivalves and from the apical to the abapical region in gastropods in order to detect every small change in the shell microstructure. The other half of each shell was crushed to a fine powder using an agate mortar and pestle.

To define the mineralogical composition, powdered shells were analyzed by X-ray powder diffraction (XRD) using a Panalytical X'pert Powder Diffractometer at the Dipartimento di Scienze della Terra of the University of Milan, Italy. The powders (mean size = ~50–60 μm) were inserted in a back-mounting sample holder to reduce preferential orientation. When the amount of the

https://doi.org/10.1017/qua.2022.62 Published online by Cambridge University Press

sample was not enough to fill the standard sample holder, the powder was deposited on a zero-background plate. The X-ray tube (Cu Kα wavelength) was set at 40 kV and 40 mA, and data were collected between 5° 2θ and 90° 2θ, with a step size of about 0.02° 2θ and a counting time per step of 30 seconds. The incident slit was fixed at 1/2°, with an antiscatter of 1/2°; the detector used was a multistrip X'Celerator. Table 1 gives the approximate weight percentages of aragonite and calcite in the samples. In order to evaluate the weight percent of a component in a mixture by X-ray powder diffraction, it is necessary to know the mass absorption coefficient of the mixture, which is unknown, as it is defined as the weighted (as a function of the components' masses) average of the mass absorption coefficients of the components. In this case, the two components are polymorphs, have the same chemical composition and therefore the same mass absorption coefficient, i.e. the mass absorption coefficient of the mixture is the same as the one of its components. Hence, it is possible to evaluate the weight percent of the components using the integrated intensity of the peaks, in the following way: the area of calcite main peak (with d = 3.037 Å) is divided by the sum of the peak areas of calcite and aragonite (with d = 3.401 Å), then multiplied by 100.

To analyze the oxygen and carbon isotope shell composition, about 200–300 μg of powdered calcium carbonate from each sample was analyzed using an automated carbonate preparation device (GasBench II) connected to a Delta V Advantage (Thermo Fisher Scientific Inc., Waltham, Massachusetts, USA) isotope-ratio mass spectrometer (IRMS) at the Dipartimento di Scienze della Terra of the University of Milan, Italy. Isotope values ($\delta^{18}O$, $\delta^{13}C$) are reported as per mil (‰) deviations of the isotope ratios ($^{18}O/^{16}O$, $^{13}C/^{12}C$) calculated to the Vienna Pee Dee Belemnite (VPDB) scale using a within-run internal laboratory standard (MAMI) calibrated against the International Atomic Energy Agency 603 standard (IAEA-603) and NBS-18 standard. Analytical reproducibility (1σ) for these analyses was better than 0.2‰ for $\delta^{18}O$ and $\delta^{13}C$ values.

Aside from the multi-methodological analyses performed on some selected shells listed above, we counted the number of burned shells and the total shell number per each burned species found in the two circular structures B5 and B9 (Table 2). Also, the purpose of use for each species has been determined (food consumption, ornaments, etc.).

RESULTS

Shell external appearance

Burned shells, i.e., specimens showing a dark-colored shell, were found in circular structures B5 (68 specimens) and B9 (11 specimens), with both bivalve and gastropod species represented (Table 2). Dark-colored shells generally appeared more fragile and brittle compared to light-colored specimens, and when they were crushed to powder with pestle and mortar, they broke easily, whereas light-colored specimens were harder and more difficult to pulverize. Certain specimens of *Perna perna* (BS-304), *Naria* sp. (BS-202), and *Oliva bulbosa* (BS-114) were very brittle and easy to grind. Also, the outer shell layer tended to detach from the rest of the shell and separated easily from the inner shell layer (Fig. $2G_2$, N_2) in *O. bulbosa* specimen BS-114 and *Naria* sp. specimen BS-202. The *O. bulbosa* specimen BS-114 also showed a residual color zig-zag pattern that was not evident in the other dark-colored specimen of the same species (BS-40); this zig-zag pattern is clearly observable in light-colored specimens of *O. bulbosa* (BS-45, BS-80), one of which also displays a glossy shell surface (specimen BS-80; Fig. 2O).

Shell microstructure

Gastropod and bivalve shells were analyzed using a SEM to see if there were differences in the microstructure between dark- and light-colored shells (Figs. 3–7; Table 1). The terminology used here follows Carter et al. (2012) and Carter and Sato (2020).

Oliva bulbosa (Fig. 3): light-colored specimens (BS-45, BS-80) show a well-defined crossed-lamellar microstructure occurring as alternating layers of linear or branching crossed lamellae and irregular, complex crossed lamellae (Fig. 3A–D). The crossed lamellar layers alternate irregularly without any specific organization or pattern. The dark-colored specimen of *O. bulbosa* (BS-114) shows a recrystallized shell with the original crossed-lamellar microstructure replaced by irregular prisms of variable size (Fig. 3E, F); in some places, the organization in first-order lamellae is still visible, but second- and third-order lamellae are not present and were replaced by prisms. The *O. bulbosa* specimen BS-40, although showing a dark brown color, has a shell composed of crossed lamellae (Fig. 3G), like those of the light-colored specimens, but in a few places (mainly in the outer layer), recrystallization occurred and irregular prisms and second- and third-order elements coalesced (Fig. 3H).

Conus sp. (Fig. 4): light-colored specimens (BS-124, BS-168) show a well-defined crossed-lamellar microstructure similar to that of *O. bulbosa* specimens, with irregularly alternating layers of linear and branching crossed lamellae and irregular, complex crossed lamellae present (Fig. 4A, B). The dark-colored *Conus* sp. specimen (BS-166) has a recrystallized shell where the original crossed-lamellar microstructure has been replaced by irregular prisms of variable size (Fig. 4C,D); in many places, the organization of first-order lamellae is still visible (Fig. 4D), although second- and third-order lamellae were not preserved. In contrast, although having a dark-colored shell, *Conus* sp. specimen BS-126 has a well-preserved microstructure consisting of simple and irregular complex crossed lamellae (Fig. 4E, F).

Naria sp. (Fig. 5A–D): the light-colored specimen (BS-193; Fig. 5A, B) has a distinct and pristine crossed-lamellar microstructure occurring as alternating layers of linear and branching crossed lamellae and irregular, complex crossed lamellae, and growth lines in the outer shell layer are also distinct. In a few places in this specimen, second- and third-order lamellae coalesced, forming larger units. *Naria* sp. specimen BS-202 has a dark-colored shell, but it is mainly composed of crossed lamellae (linear, branching, and complex), although recrystallized portions occur in a few places (rarely in the outer layer, more frequently in the inner layer), with irregular prisms of different sizes and second- and third-order elements coalescing (Fig. 5C, D).

Perna perna (Fig. 5E–H): the light-colored specimen of *P. perna* (BS-303) shows a thin outer prismatic layer, and the middle and inner layers have a sheet nacre microstructure with distinct tablets arranged in parallel (Fig. 5E, F), separated by an irregular, prismatic pallial myostracum. In contrast, the dark-colored specimen of *P. perna* (BS-304) has several fractures filled by recrystallized irregular prisms (Fig. 5G) and relicts of nacre sheets are still visible, but the boundaries between tablets are not defined because they have coalesced into an irregularly shaped assemblage made of several single tablets (Fig. 5H).

Anadara uropigimelana (Fig. 6): the three analyzed specimens show different degrees of preservation from a shell retaining the

https://doi.org/10.1017/qua.2022.62 Published online by Cambridge University Press

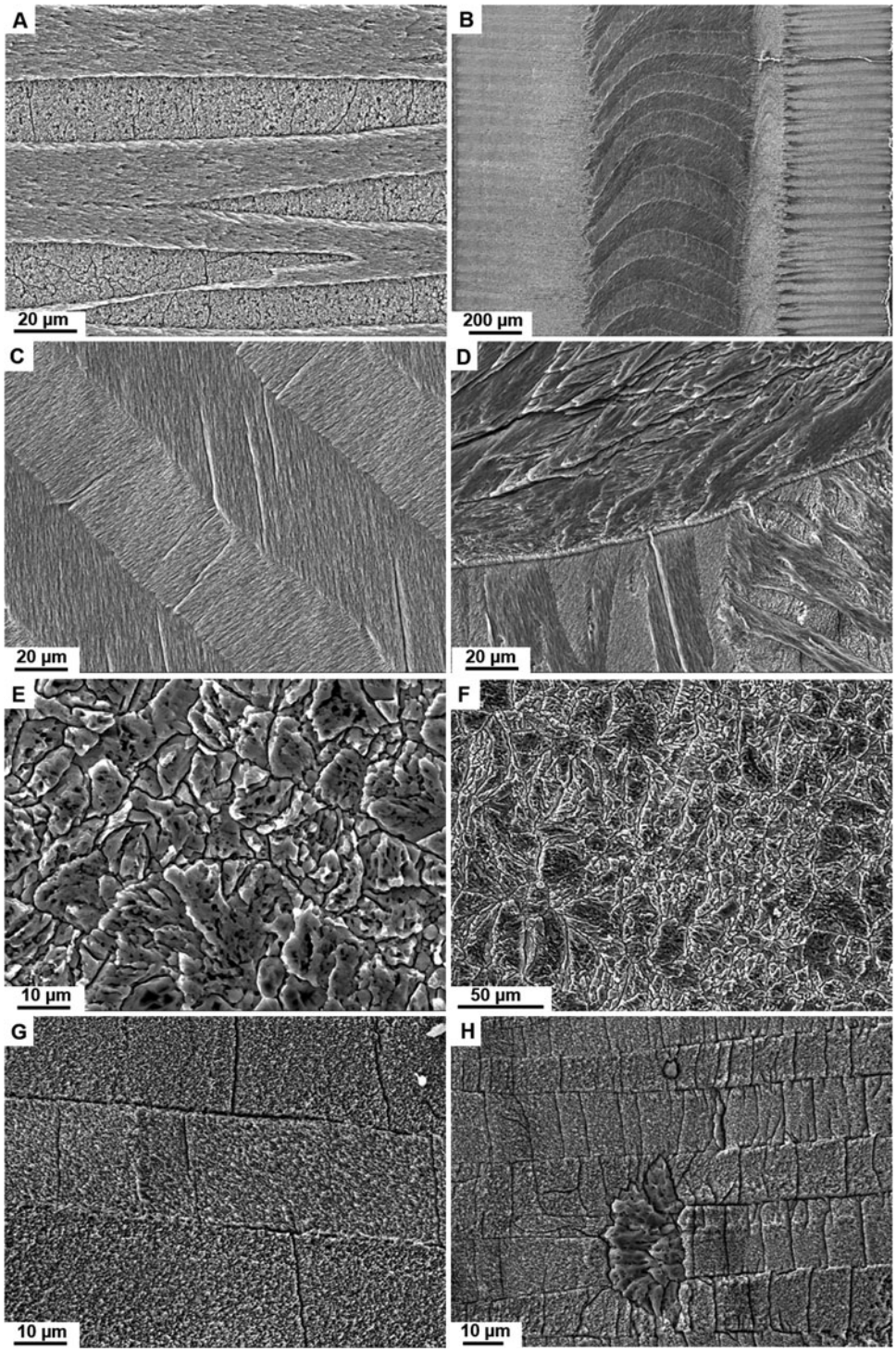

Figure 3. Shell microstructure of *Oliva bulbosa* specimens. (A–D) Well-preserved crossed lamellae occurring as alternating layers of linear (A, C) or branching crossed lamellae (B) and irregular, complex crossed-lamellae (D) (A, B: BS-45, C, D: BS-80). (E, F) Original crossed lamellar microstructure is replaced by irregular prisms of variable sizes (BS-114); (G, H) well-preserved crossed lamellae with some irregular prisms seen in (H) (BS-40).

original microstructure (BS-300; Fig. 6A, B) to a partially recrystallized shell (BS-301; Fig. 6C, D) to a nearly totally recrystallized shell (BS-302; Fig. 6E, F). The light-colored specimen of *A. uropigimelana* (BS-300) shows different layers crossed by tubules: an outmost composite prismatic layer, an outer linear and branching crossed-lamellar layer, an inner complex crossed-lamellar layer, and an irregular prismatic pallial myostracum (Fig. 6A, B). The altered specimen of *A. uropigimelana* (BS-302) has a shell mainly composed of irregular prisms of variable size (Fig. 6E, F), although well-preserved first-, second-, and third-order crossed lamellae appear in few areas of the shell together with recrystallized prisms (Fig. 6E), as well as tubules penetrating the layers. An intermediate situation occurs in the *A. uropigimelana* specimen BS-301, where its shell consists of linear, branching, and

https://doi.org/10.1017/qua.2022.62 Published online by Cambridge University Press

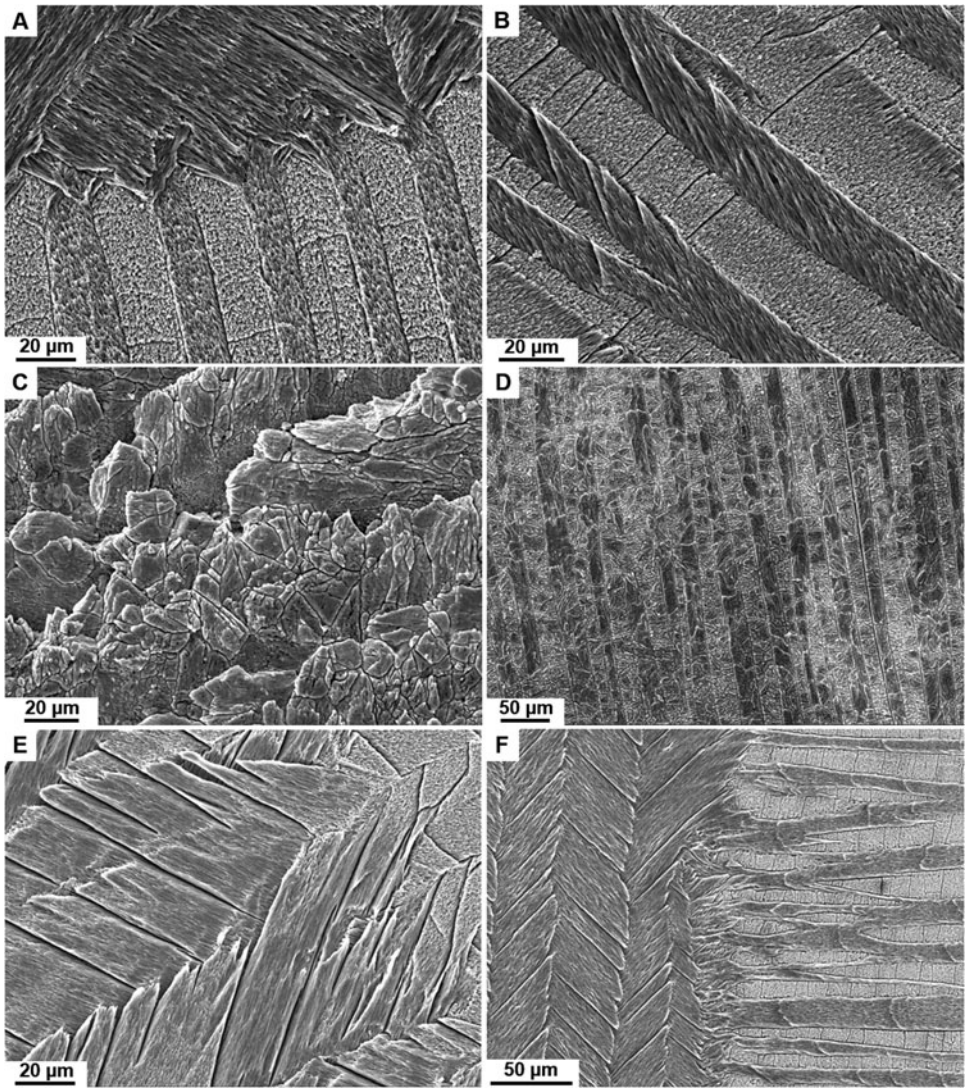

Figure 4. Shell microstructure of *Conus* sp. specimens. (A, B, E, F) Well-defined crossed lamellar microstructure showing alternating layers of linear and branching crossed lamellae (A: BS-124, B: BS-168, E, F: BS-126); (C, D) the original crossed-lamellar microstructure is replaced by irregular prisms of variable size, although in many places, the organization of first-order lamellae is still clearly visible (BS-166).

complex crossed lamellae penetrated by tubules, but few recrystallized prisms are present (Fig. 6C, D).

Saccostrea cucullata (Fig. 7): the light-colored portion of specimen BS-261 shows a well-preserved foliated microstructure, both regularly and complex crossed-foliated (Fig. 7A, B). The dark portion of the shell still preserves well-defined folia, but single laths coalesced, forming larger units (Fig. 7C, D); however, totally recrystallized areas with prisms are lacking. The transition between these two portions is gradual, with the number of coalescent laths increasing toward the dark portion of the shell.

Mineralogical composition

X-ray diffraction analysis allows differentiation between aragonite and calcite. This is particularly important to detect if originally aragonite shells were transformed into calcite due to high temperatures (Figs. 8, 9; Table 1). Also, as calcite and aragonite are the only two components of the mixture and they have the same chemical composition, the approximate weight percentages of aragonite and calcite in the samples have been also calculated (Table 1; see Methods for detailed explanation of the procedure).

Among the gastropod shells originally composed of aragonite, specimens fully conserving this mineralogy are BS-45 (*Oliva bulbosa*), BS-124, BS-126, and BS-168 (*Conus* sp.), whereas one specimen (BS-114, *O. bulbosa*) has a 100% calcite shell. Intermediate conditions, i.e., different proportion of aragonite and calcite within the same shell, are found in *O. bulbosa* specimens BS-40 (83% aragonite, 17% calcite) and BS-80 (94% aragonite, 6% calcite), *Conus* sp. specimen BS-166 (5% aragonite, 95% calcite); and *Naria* sp. specimens BS-193 (98% aragonite, 2% calcite) and BS-202 (84% aragonite, 16% calcite).

Among originally aragonitic bivalves, specimens with a 100% aragonite shell are BS-300 (*Anadara uropigimelana*) and BS-303 (*Perna perna*), whereas a specimen with a fully calcite shell is BS-304 (*P. perna*). Specimens BS-301 and BS-302 (*A. uropigimelana*) show intermediate conditions, i.e., different proportion of aragonite and calcite within the same shell, with 85% aragonite and 15% calcite and 13% aragonite and 87% calcite, respectively. The originally calcite shell *Saccostrea cucullata* is composed in both light and dark-colored portions by 100% calcite (Fig. 9 B).

https://doi.org/10.1017/qua.2022.62 Published online by Cambridge University Press

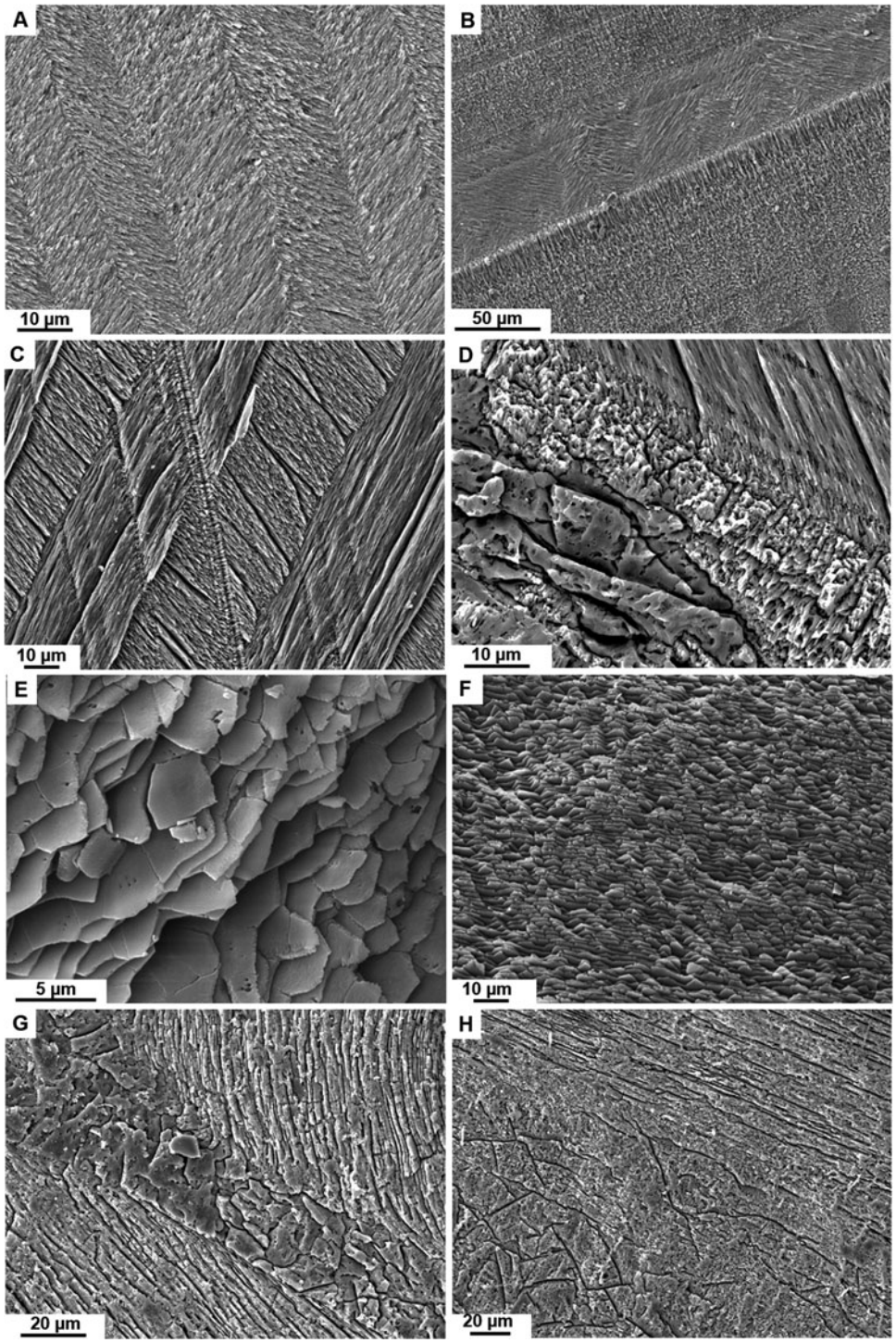

Figure 5. Shell microstructure of (A–D) *Naria* sp. and (E–H) *Perna perna*. (A, B) well-defined linear crossed lamellae (BS-193); (C, D) well-preserved crossed lamellae with some recrystallized portions (BS-202); (E, F) pristine sheet nacre tablets (BS-303); (G, H) relict nacre sheets still visible, but tablets started to coalesce to create an irregular-shaped assemblage; (G) several fractures filled by recrystallized irregular prisms (BS-304).

Shell stable-isotope composition

All shell stable-isotope analyses are reported in Table 1. Specific findings are given below broken out by taxon.

Oliva bulbosa: A trend toward lower $\delta^{18}O$ values was observed from fully aragonite to fully calcite specimens. Specimen BS-45 (100% aragonite) had a $\delta^{18}O$ value of +0.23‰, whereas specimen BS-114 (100% calcite) had a $\delta^{18}O$ value of −0.27‰, with variation in the $\delta^{18}O$ value between the two = 0.50‰. Specimens having a mixture of aragonite and calcite in their shells had a $\delta^{18}O$ value of +0.17‰ (BS-80) and −0.06‰ (BS-40). No trend was observed in the carbon isotope composition of the analyzed specimens; the highest value found was +1.47‰ (BS-45), while the lowest was +0.38‰ (BS-80).

https://doi.org/10.1017/qua.2022.62 Published online by Cambridge University Press

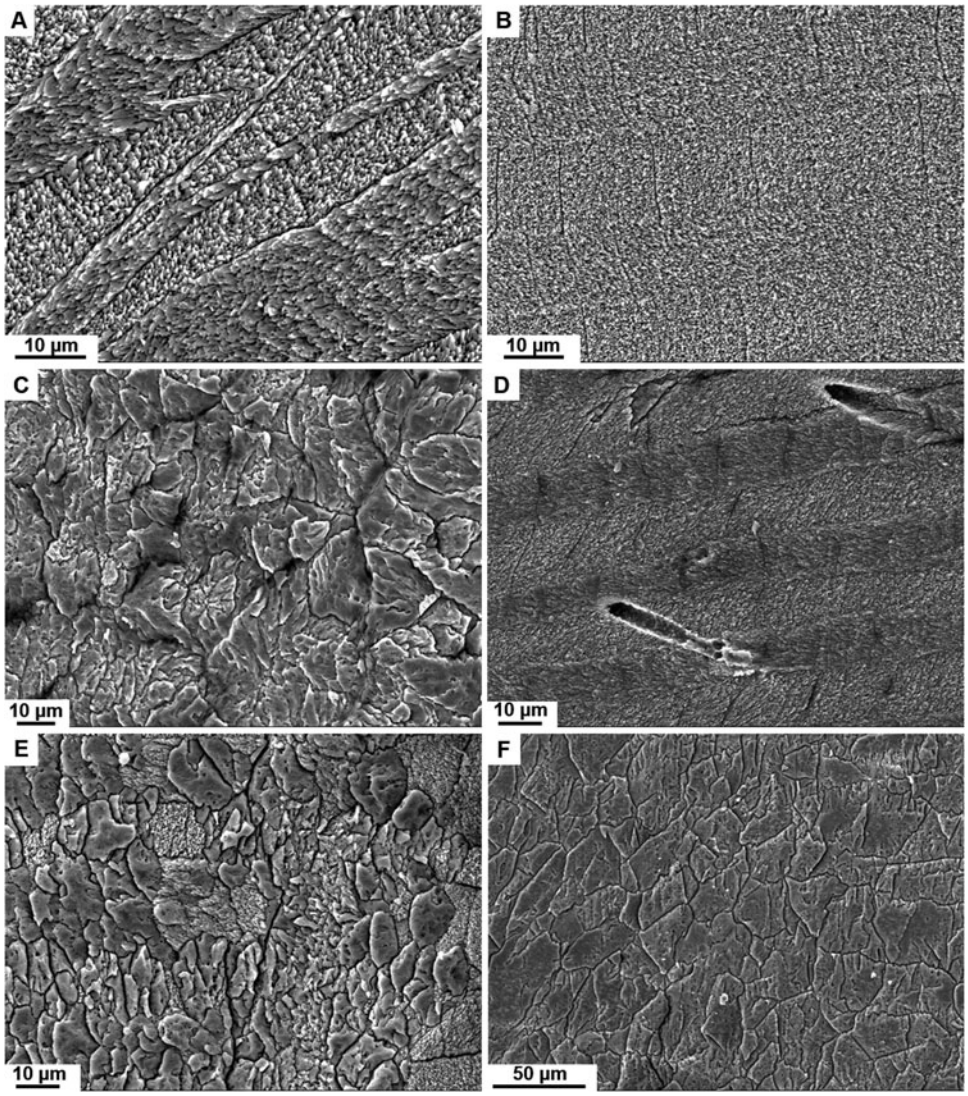

Figure 6. Shell microstructure of *Anadara uropigimelana* specimens. (A, B) Preserved linear and branching crossed lamellae (BS-300); (C, D) linear crossed lamellae penetrated by tubules (D), although recrystallized prisms are present (C) (BS-301); (E, F) irregular prisms of variable size; well-preserved crossed lamellae appear in few areas along with recrystallized prisms (E) (BS-302).

Conus sp.: In 100% aragonite specimens, $\delta^{18}O$ values ranged between +0.27‰ and +0.40‰, whereas in the fully calcite specimen, the $\delta^{18}O$ value was −0.15‰, with a difference in $\delta^{18}O$ values between completely aragonite and calcite specimens of 0.42–0.55‰. The lowest $\delta^{13}C$ value found was +0.42‰ (BS-124), whereas the highest $\delta^{13}C$ value was +2.5‰ (BS-126); intermediate $\delta^{13}C$ values were found in specimens BS-166 and BS-168 of +1.27‰ and +1.34‰, respectively.

Naria sp.: The $\delta^{18}O$ values from specimens BS-193 and BS-202 were +0.24‰ and +0.86‰, respectively, with a variation in $\delta^{18}O$ values of 0.62‰. The $\delta^{13}C$ values were similar between the two specimens, with a $\delta^{13}C$ value of +2.62‰ for BS-193 and a $\delta^{13}C$ value of +2.31‰ for BS-202.

Perna perna: A variation of 1.90‰ for $\delta^{18}O$ values and 2.32‰ for $\delta^{13}C$ values was found between a fully aragonite (BS-303) and a fully calcite (BS-304) specimen.

Anadara uropigimelana: All of the analyzed specimens had low $\delta^{18}O$ values, ranging from a $\delta^{18}O$ value of −0.55‰ in the 100% aragonite specimen (BS-300) to a $\delta^{18}O$ value of −0.85‰ in the mostly calcite specimen (BS-302), showing a difference in a $\delta^{18}O$ values of 0.30‰. The highest $\delta^{18}O$ value was found in BS-301 ($\delta^{18}O = -0.33$‰). A trend toward lower $\delta^{13}C$ values is observed from fully aragonite to mostly calcite specimens. Specimen BS-300 (100% aragonite) had a $\delta^{13}C$ value of −0.16‰, whereas BS-302 (87% calcite) had a $\delta^{13}C$ value of −0.86‰, with a difference in the $\delta^{13}C$ isotope composition of 0.70‰.

Saccostrea cucullata: The light portion of the shell specimen shows a $\delta^{18}O$ value of −0.89‰ whereas the dark portion has a $\delta^{18}O$ value of −0.31‰, recording a variation in $\delta^{18}O$ of 0.58‰. The $\delta^{13}C$ values are similar in the two portions of the specimen, with a $\delta^{13}C$ value of +0.82‰ for the light portion and a $\delta^{13}C$ value of +0.63‰ for the dark portion.

DISCUSSION

Reconstructing temperatures experienced by mollusk shells

Aragonite is a metastable form of calcium carbonate at ambient pressure and temperature conditions, but, as diagenetic alteration proceeds, it is commonly replaced by thermodynamically stable

https://doi.org/10.1017/qua.2022.62 Published online by Cambridge University Press

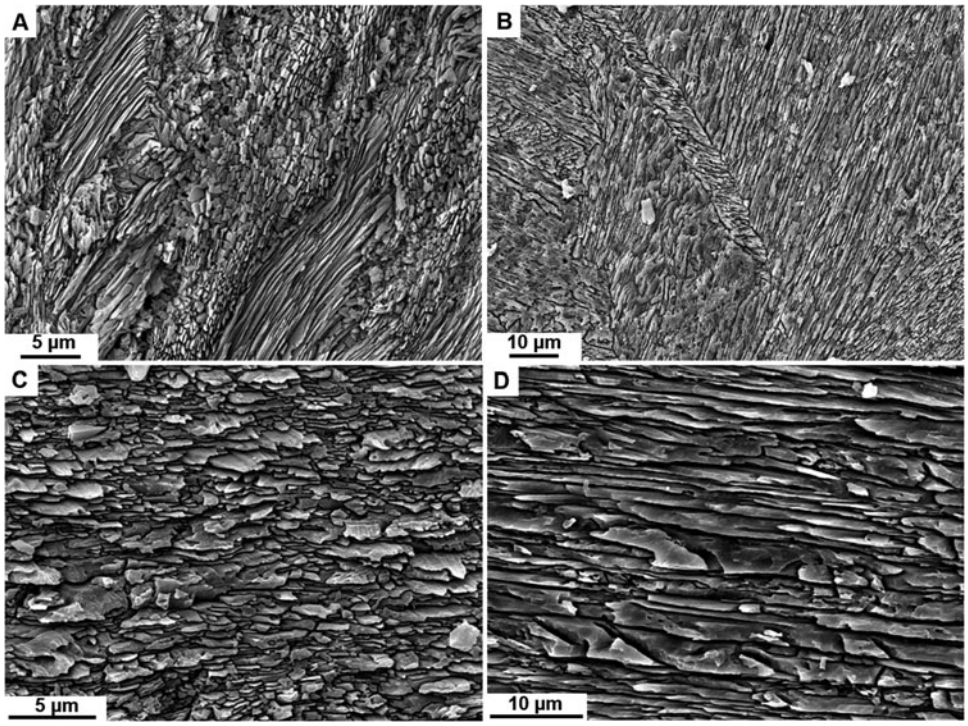

Figure 7. Shell microstructure of *Saccostrea cucullata* specimen. (A, B) Well-preserved regular and complex crossed-foliated fabric (BS-261W); (C, D) single laths coalesced to form larger units (BS-261B).

calcite (see Casella et al., 2017, and references therein). Experimental data from mollusk shells suggest that when this reaction is fluid-mediated, it begins at temperatures around 175–200°C (Lécuyer, 1996; Casella et al., 2017), and can occur at Earth surface temperatures on geological time scales. Conversion of bioaragonite into inorganic calcite also takes place as a solid-state reaction, but generally at higher temperatures (≥300°C; Milano et al., 2016, 2018; Staudigel and Swart, 2016; Milano and Nehrke, 2018). Several studies on modern mollusk shells and fish otoliths that mimicked ancient cooking practices simulated a thermally induced diagenesis associated with heat exposure, where high temperatures accelerated a process that naturally would require thousands of years (e.g., Andrus and Crowe, 2002; Larsen, 2015; Li et al., 2015; Milano et al., 2016, 2018; Müller et al., 2017; Lindauer et al., 2018; Aldeias et al., 2019). Generally, besides conversion of bioaragonite into inorganic calcite, the heating process causes changes in the shell microstructure, such as coalescence of basic shell structural units into much larger, joint aggregates, with a very heterogeneous and disordered spatial arrangement, and/or the formation of large and irregular calcite crystals (e.g., Milano et al., 2016, 2018; Lindauer et al., 2018). Analysis of shell microstructural variations and assessment of the relative amounts of aragonite versus calcite may help to determine the temperature range to which a shell from an archeological deposit was exposed, although it is not possible to reconstruct the duration of the process (Milano et al., 2018; Aldeias et al., 2019).

Light-colored shells

Shells that can provide information about exposure temperature are those that looked burned; therefore, the following discussion will mainly focus on shells with this appearance. However, some considerations are necessary for shells that, based on external appearances, look pristine. Specimens belonging to *O. bulbosa* (BS-45), *Conus* sp. (BS-124, BS-168), *A. uropigimelana* (BS-300) and *P. perna* (BS-303) all have a light-colored shell (beige, light brown), original microstructure and mineralogy, and a high resistance to breakage, suggesting that they were well-preserved and were not affected by natural diagenesis. According to Milano et al. (2016, 2018) and Müller et al. (2017), no modification in shell microstructure or mineralogy was observed if shells were exposed to a temperature less than 300°C. Therefore, the mollusk shells analyzed for this study may have not experienced any heating or, if so, they were only heated to a temperature below 300°C, where no visible changes in the external coloration, microstructure, and mineralogy occur. An exception is represented by the specimen of *Conus* sp. (BS-126) that was considered a burned shell based on its gray external surface; however, the results of our multi-approach analysis show that this specimen retained its original crossed-lamellar microstructure and aragonite mineralogy, as seen in the not-burned shells. We hypothesize that this specimen was probably exposed to temperatures near 300°C because there was visible alteration of the external surface but there was no change in microstructure or mineralogy, which requires a higher temperature (e.g., Larsen, 2015; Milano et al., 2018).

Dark-colored shells

Previous studies have highlighted the fact that different shell microstructures may respond differently to heating. This is due to different organic content and organic matrix composition affecting the aragonite-to-calcite conversion temperature for different shell microstructures (e.g., Milano and Nehrke, 2018; Aldeias et al., 2019). For this reason, we chose to organize the discussion of burned shells based on shell microstructure.

Although crossed lamellae are one of the most common microstructures in mollusks (e.g., Rodriguez-Navarro et al.,

https://doi.org/10.1017/qua.2022.62 Published online by Cambridge University Press

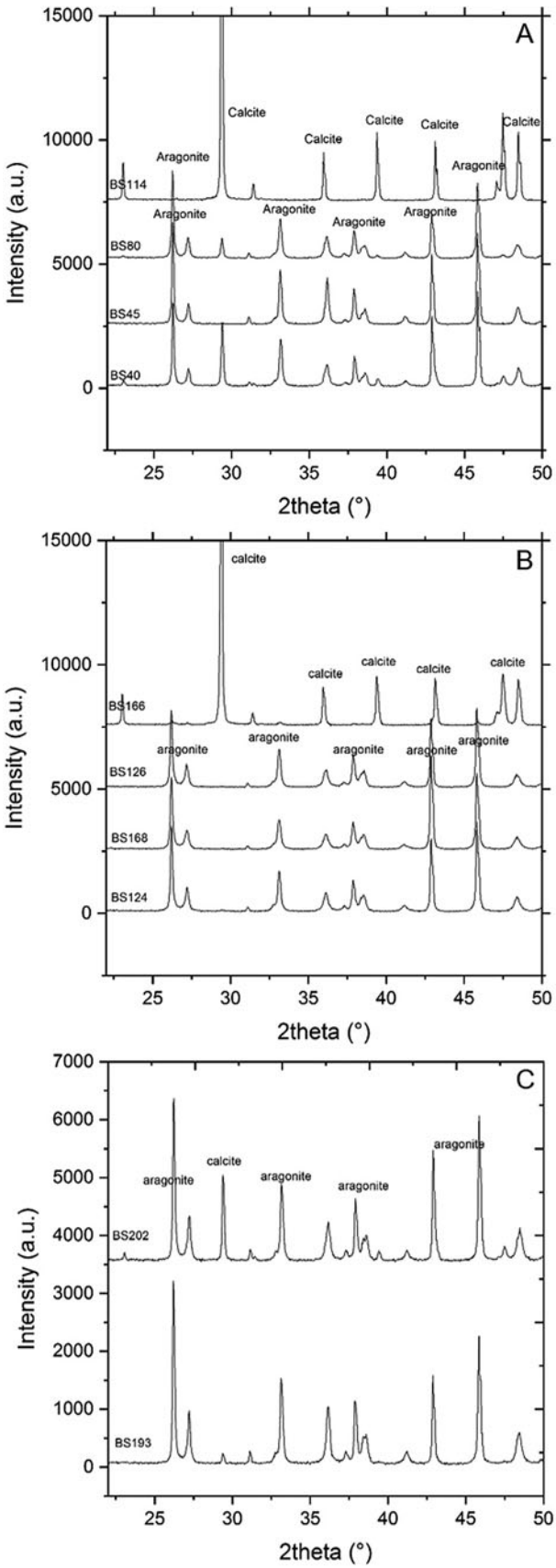

Figure 8. Diffractograms for gastropod specimens showing main peaks for calcite and aragonite with individual spectra labeled with specimen field numbers for: (A) *Oliva bulbosa*; (B) *Conus* sp.; (C) *Naria* sp. a.u.: arbitrary units.

2012; Almagro et al., 2015; Crippa et al., 2020), few studies have examined the response of this fabric to heating. Studies have focused mainly on the effects of heating on external coloration and the temperature at which the phase transformation occurs, but detailed studies on this microstructure are lacking. Moon et al. (2021) noted no evidence of secondary textures associated with transformation of aragonite to calcite in modern specimens of *Spisula solidissima* (Dillwyn, 1817) heated at 200°C. Li et al. (2015) observed that in modern specimens of the gastropod *Busycon carica* (Gmelin, 1791) heated to 310°C, aragonite and crossed lamellae are well-preserved, but at 500°C, calcite is detected, although shells retained their crossed-lamellar structure despite the phase transformation. According to Li et al. (2015), bioaragonite starts to transform into calcite at 407°C. Aldeias et al. (2019) analyzed modern specimens of *Cerastoderma edule* (Linnaeus, 1758), which has most of its shell composed of crossed lamellae, and documented that the polymorphic conversion from aragonite to calcite occurs between 250°C and 500°C. According to these studies and our observations, we can infer that shells with crossed-lamellar microstructure from the HAS1 settlement experienced two ranges of temperatures.

First, some shells experienced temperatures between 250–500°C. These shells have a dark external coloration (light to dark brown, light gray), a different proportion of aragonite and calcite, and retain an original crossed-lamellar microstructure but show third-order lamellae losing geometric definition and starting to coalesce, and the occurrence of irregular prisms suggesting the beginning, but not the completion, of the recrystallization process. This temperature range applies to shells of *O. bulbosa* (BS-40, BS-80), *Conus* sp. (BS-166), *Naria* sp. (BS-193, BS-202) and *A. uropigimelana* (BS-301, BS-302). Shells showing a higher percentage of calcite and more frequent recrystallized prisms (*Conus* sp., BS-166; *A. uropigimelana*, BS-302) were probably exposed to temperatures in the highest range of this interval.

Second, a shell of *O. bulbosa* (BS-114) was exposed to temperatures of 500°C, and shows a dark gray, 100% calcite shell with the original microstructure replaced by recrystallized prisms, suggesting that the higher temperature experienced led to a complete transformation of aragonite into calcite. Notwithstanding this heat exposure, the external color ornamentation on this specimen is surprisingly still preserved.

Nacre has a similar response to heat to that of crossed lamellae, and seems to retain its integrity until 500°C. Milano et al. (2016, 2018) and Milano and Nehrke (2018), who analyzed the inner nacreous layer of modern specimens of *Phorcus lineatus* (da Costa, 1778) and *Ph. turbinatus* (Born, 1778), observed that at 500°C, coalescence of nacre tablets increases and calcite is the main mineral phase, whereas at lower temperatures, the mineralogy of the shells was still aragonite. The *P. perna* specimen BS-304 has a dark gray to black shell, and is entirely composed of calcite with many fractures filled by recrystallized prisms; nacre tablets are still visible, but they often have coalesced. We speculate that the temperature experienced by this shell was ≥500°C.

It should be noted that all previous experiments to detect shell mineralogical changes with heating were performed on modern aragonite shells and not on calcite shells mainly because of the ease of detecting changes as aragonite transforms into calcite. Larson (2015) analyzed a specimen of *Ostrea lurida* Carpenter 1864, which has a foliated calcite shell. The author observed that this shell retained its calcite mineralogy for each temperature to which it was heated (300°C, 400°C, 500°C). However, the author did not examine the shell microstructure. In the specimen

https://doi.org/10.1017/qua.2022.62 Published online by Cambridge University Press

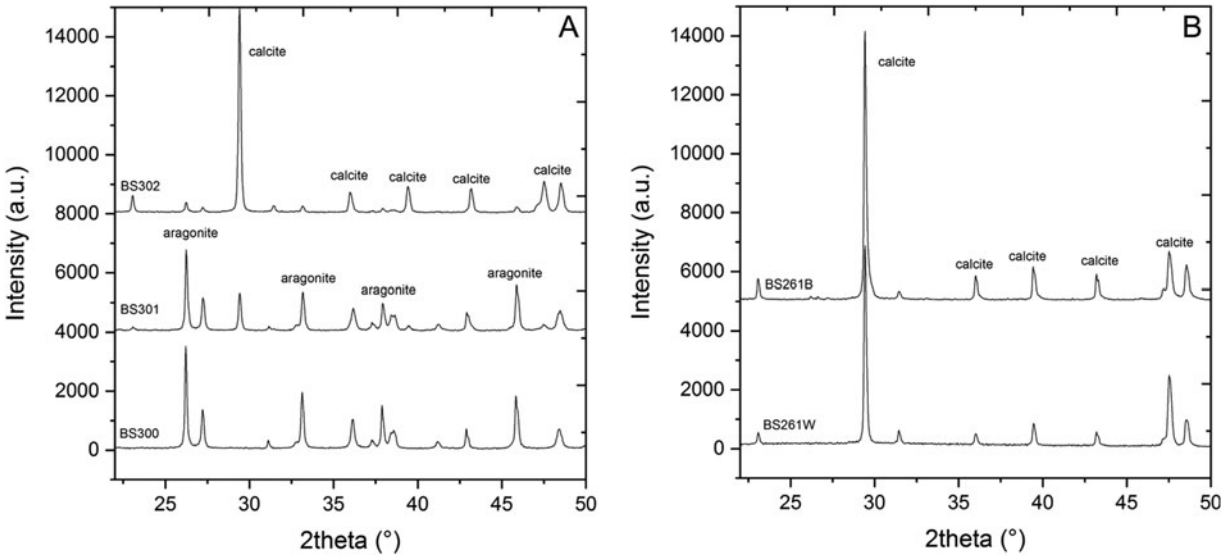

Figure 9. Diffractograms of bivalve specimens showing the main peaks of calcite and aragonite with individual spectra labeled with specimen field numbers for: (A) *Anadara uropigimelana*; (B) *Saccostrea cucullata*. a.u.: arbitrary units.

of *S. cucullata* we analyzed, we found a difference in the microstructure between light- and dark-colored shell portions; however, the mineralogy detected was still calcite, but using XRD analysis, it is not possible to discern between primary or secondary calcite. The light-colored part of the *S. cucullata* shell shows pristine folia, whereas the dark part has single laths that had coalesced to form larger units, suggesting that this part of the shell was likely subjected to high temperatures, as also indicated by the dark coloration. Unfortunately, in the absence of studies on modern calcite specimens simulating thermally induced diagenesis, it is not possible to infer an exposure temperature for this specimen of *S. cucullata* based solely on shell microstructural and mineralogical changes. Although the majority of mollusk species have an aragonite shell, many paleoenvironmentally useful bivalves and gastropods found in archeological sites have a calcite shell (e.g., *Patella;* Ferguson et al., 2011; Nouet et al., 2015). Future research should address this gap in our understanding of the behavior of calcite shells (microstructure, mineralogy, stable isotopes) under different heating treatments.

Cooking or fire?

The multidisciplinary analyses performed on specimens from the HAS1 settlement resulted in three different temperature ranges shells were exposed to: ≤300°C, 250–500°C, and ≥ 500°C. Shells in archeological sites can be exposed to higher temperatures through cooking/disposal processes and/or if they are involved in a fire (natural or human-caused). Cooking by controlled fire is the most common situation in which mollusk shells experienced heating because this procedure was used by ancient populations to maximize energy gain and improve food digestibility, as well as facilitating the extraction of edible portions of the mollusk (e.g., Wrangham, 2009; Wrangham and Carmody, 2010; Milano et al., 2018). Together with intentional fires, wildfire events can occur in archeological sites. However, a distinction between intentional and unintentional fires cannot be detected based solely on shell thermal responses (Milano et al., 2018).

As noted above, the mollusk shells we analyzed indicated a heterogeneous thermal history. According to Aldeias et al. (2019), who simulated different fire-cooking techniques, when a fire was set on top or underneath a pile of shells, the heat diffusion affected single specimens differently according to their position with respect to the heat source, resulting in a mixture of aragonite and calcite shells. Staudigel et al. (2019) interpreted the nonuniform thermal history recorded in the bivalve shells they analyzed as deriving from different scenarios, including the discarding of uncooked shells to account for the presence of pristine shells, the use of various cooking techniques that generated different thermal histories for different shells, or the use of a single cooking procedure whereby shells were unevenly heated. These interpretations may be also considered to explain the heterogeneous thermal response observed in the specimens we examined. However, burned shells found in the circular structures B5 and B9 are not only from edible species (Table 2). Shells were probably used for different purposes: some shells resulted from food consumption, such as *P. perna*, *S. cucullata*, *Ostrea* sp., *A. uropigimelana*, *Babylonia spirata* (e.g., Carenti and Wilkens, 2008), other as ornaments, such as *Oliva bulbosa*, *Conus* spp., *Naria* spp., *Purpura panama* (e.g., Carenti and Wilkens, 2008; Lischi, 2018, 2020). We also did not find a relationship between the number of burned shells and species. When we examined the same species, the number of burned shells versus total shell number is similar, suggesting that the heating affected different species used for different purposes in the same way (Table 2). According to Aldeias et al. (2019), either roasting or boiling mollusks involved preparation of several specimens at the same time because cooking is a substantially more cost-efficient way of processing mollusks than the time-consuming task of cracking each valve individually. The number of burned shells from edible species found in the two circular structures B5 and B9 is low; thus, it seems unlikely that the main cause of the burning of these specimens was only heating for food consumption.

Burned shells have also been found inside the two megalithic circular structures where wooden poles and the rooves were found completely carbonized in situ (Fig. 10). Therefore, our

https://doi.org/10.1017/qua.2022.62 Published online by Cambridge University Press

Figure 10. Carbonized wooden beam found in stratigraphic unit US54 in circular structure B9. The length of the beam is ~20 cm.

shell data and other evidence available conform better with intentional or accidental fires, rather than cooking or disposal processes. If the presence of carbonized in situ wooden poles led us to suppose that a fire occurred in the settlement, then it is only with our multi-methodological analysis of the shells, complemented with a correct identification of specimens at specific level and an investigation of shell use or consumption by the local population, that this hypothesis has been confirmed, and that additional data about this event are now known (e.g., reconstructed shell-exposure temperatures, specimen distance from the heat source, discrimination between different types of shell heating).

Temperatures reached during a fire can be very high, but it must be considered that within a fire, temperatures vary greatly depending on the type of fuel used, its amount, and the frequency of refueling, as well as the varying with the duration of the fire, which can be rapid or long-lasting (Aldeias et al., 2016). For instance, in the experiments performed by Aldeias et al. (2019) pine wood and needles were used as fuel and reached temperatures up to 800°C, whereas grass material is known to burn at lower temperatures (maximum ~320°C; see also Table 2 in Aldeias et al., 2016 for an overview on maximum fire temperatures depending on fuel used). According to Aldeias et al. (2016), fire heats underlying sediments through conduction, and heat is transmitted gradually downward through the sediment. Initially, heat is transmitted quickly to the sediment, then it slows progressively as sediments reach thermal equilibrium. Thus, sediments that are directly below a heat source are heated more quickly and to a higher extent than sediments located adjacent to or outside a heat source, thus these sediments will show little or no thermal alteration.

The heterogeneous thermal response of the studied shells thus may be explained by taking into account the distance of the specimens from the heat source. Aldeias et al. (2019) observed that when originally aragonite shells undergo a complete conversion to calcite mineralogy, high temperatures had to have been maintained long enough to result in widespread transformation of shell material from aragonite to calcite. This conversion from aragonite to calcite in shell material is more consistent with events such as throwing shells into an active fire for disposal, or if the shells were part of the substrate underlying a fire, rather than cooking. As observed by Aldeias et al. (2019), roasting techniques primarily involved rapid fires where the temperature of the fire can oscillate between ~400°C and ~900°C, but temperatures above 400°C only occur locally in association with cooking mollusks. Generally, much lower temperatures are needed for roasting, otherwise the mollusk is burned instead of cooked.

These previous observations allow us to suppose that the entirely calcite shells found in the HAS1 settlement may have been located in close proximity to a heat source (e.g., in the substrate underlying a fire) where temperatures were high enough to favor the aragonite-to-calcite conversion; shells having a different proportion of aragonite to calcite or retaining the original aragonite mineralogy may have been sited laterally or were buried deeper in the sediments with respect to the heat source. Experimental work by Aldeias et al. (2016) estimated that conversion temperatures can be reached in sediments up to 6 cm deep. We cannot exclude the possibility that some shells that were directly exposed to the fire and/or for a longer time may have become ash and been completely lost due to the high temperatures they were subjected to (>700°C). The possibility of identifying the range of temperatures at which the shells were exposed can give us a precise indication of where the specimens were at the time of the fire; however, this may not have a direct relation to where they were found in the stratigraphic layer (e.g., due to later collapses or other processes).

Effects of burning on shell isotope composition

Previous studies have demonstrated that heat exposure can drastically alter the original isotope composition in otoliths and mollusk shells (Andrus and Crowe, 2002; Milano et al., 2016, 2018). Temperatures >300°C cause a significant decrease in the original $\delta^{18}O$ values recorded in the shell material (Milano et al., 2016), which has important implications for paleoenvironmental reconstructions. However, Müller et al. (2017) and Moon et al. (2021) observed that, notwithstanding the significant alteration of oxygen isotope values, original seasonal temperature oscillations can be preserved despite heating. Although a paleoenvironmental reconstruction is not the aim of this study and will required a more detailed methodology (i.e., sclerochronology), the stable isotope analysis we performed on bulk samples can provide further data to understand the effect of heating on shell isotope composition.

To discuss the results of our stable isotope analyses, we need to consider that the examined specimens are not modern samples but were collected in an archeological site. Also, with the exception of *S. cuccullata* where powder samples were collected from two different-colored areas within the same shell, for the other species analyzed, we compared isotope signals recorded by different specimens showing varying degrees of alterations. Therefore, we need to take into account that isotope variability from shells of the same species in the HAS1 settlement may be due to the exposure to high temperatures (i.e., heating), but also may be due to different paleoenvironmental behaviors of each species, and to the fact that the specimens may have lived in different time intervals (i.e., may have been not coeval), thus the isotope values may have been recording different seawater conditions. However, if the shell stable-isotope data alone may be interpreted as a natural isotope variation recorded by the organism during its life, these data, when interpreted together with observed changes in shell external appearance, mineralogy, and microstructure, provide further evidence of the heating experienced by the shells from the HAS1 settlement.

Considering this premise, $\delta^{18}O$ values of the burned analyzed shells are always lower than those of not-burned shells, thus a general decrease in $\delta^{18}O$ values from not-burned to burned shells is observed in agreement with previous research (Milano et al., 2016). This is particularly evident in the aragonite specimens of *O. bulbosa*, *Conus* sp. and *P. perna*, which had lower $\delta^{18}O$ values by as much as 0.5‰, 0.42–0.55‰ and 1.9‰, respectively. These

https://doi.org/10.1017/qua.2022.62 Published online by Cambridge University Press

different $\delta^{18}O$ values may be due to a different species-specific alteration of the isotope ratio under heating, but also to a different temperature and duration of exposure of the shells to the heating source. As mentioned above, we cannot exclude that observed differences may also have been caused by a natural paleoenvironmental variation recorded by the mollusk during its life. If we consider heating as the main factor affecting the oxygen isotope values of burned shells, and that a shift of 1‰ in $\delta^{18}O$ values reflects a temperature change of 4.34°C (Schöne, 2013), this leads to an overestimation of the reconstructed temperatures by ~ 2.17°C, 1.82–2.39°C, and 8.20°C, respectively. When examining specimens having a mixed mineralogy but with a similar proportion of calcite and aragonite, the decrease in $\delta^{18}O$ values is not as evident (*Naria* sp. specimen BS-193 versus specimen BS-202; *A. uropigimelana* specimen BS-300 versus specimen BS-301; Table 1); this $\delta^{18}O$ decrease becomes evident when specimens of the same species, but with very different proportion of the two mineralogical polymorphs, are compared (e.g., *A. uropigimelana* specimens BS-300, BS-301 versus specimen BS-302; Table 1). Indeed, according to Larsen (2015), a shell would have to be almost completely recrystallized before a significant decrease in $\delta^{18}O$ values can be detected.

Shell carbon-isotope values are heterogeneous and, except for *P. perna* and *A. uropigimelana*, a trend toward lower values from not-burned to burned shells has not been detected. Milano et al. (2016) observed in their cooking simulations that both $\delta^{18}O$ and $\delta^{13}C$ values decreased with increasing temperatures; however, $\delta^{13}C$ exhibited an extremely high natural variation between specimens within the same treatment or control conditions. This may be explained by considering that shell carbon content derives from different sources, including dissolved inorganic carbon in the water and carbon assimilated through diet and metabolic processes (McConnaughey and Gillikin, 2008). Further analyses are required to understand if this heterogeneous response observed among the shells is due to environmental variations, heating effect, or vital effect.

In the calcite *S. cuccullata* specimen, powder samples were collected in different parts of the same shell that were light- and dark-colored. We did not observe a decrease in the $\delta^{18}O$ values between the two sampled areas, but a decrease occurred in the $\delta^{13}C$. Larsen (2015) noted that in the calcite shell of *O. lurida*, a decrease in $\delta^{18}O$ values was observed at 500°C but not at lower temperatures. This may indicate that the *S. cuccullata* specimen was probably exposed to temperature <500°C, where no significant decrease in $\delta^{18}O$ values can be observed. In particular, the slightly altered microstructure of the dark-colored portion of the shell may indicate a greater proximity of this part of the shell to the heat source. However, to confirm this hypothesis, more shells should be examined, and thermally induced diagenesis simulations on modern calcite-shelled specimens should be performed.

CONCLUSIONS

Through a multi-instrumental approach (SEM, XRD, IRMS), burned and not-burned mollusk shells from the HAS1 settlement in Dhofar, Oman, were analyzed to infer the temperatures to which these specimens were exposed, and to reconstruct the processes responsible for heating the shells. Although using the stable isotope composition of burned specimens is not recommended for paleoenvironmental purposes, these burned shells do offer a valuable source of information on the past human behaviors and human–environment interactions. One of the main conclusions of this study is that mollusk shells from the HAS1 settlement experienced three ranges of temperatures: 1) no exposure or <300°C; 2) between 250 and 500°C; and 3) ≥500°C. The heat source responsible for the heating of the shells was probably a fire that engulfed the entire settlement, as also testified to by the occurrence of carbonized wooden poles inside the circular structures where the mollusk shells were collected. During a fire event, temperatures experienced by the shells were very heterogeneous, likely due to varying proximity to the fire and duration of exposure, and changes in shell external appearance, microstructure, mineralogy, and stable isotope composition were observed equally in both edible and non-edible species. The possibility of determining shell exposure temperature and distance from a heat source is a potentially useful piece of data for identifying fire events in contexts where the heat source may be uncertain, with little evidence of burning or lack of other types of burned materials, such as wooden poles.

Our multi-approach analysis of burned mollusk shells, paired with a greater understanding of shell changes under heating provided by controlled modern experiments, is thus very useful to shed light on important events occurring in archeological sites. The identification of events such as fires destroying entire settlements has important implications in understanding past human behaviors, human dispersal, or relationships existing between different groups of humans in the area. Our case study thus can be used as a reference for other similar studies to help in discovering fire events in archeological sites.

A multi-methodological approach is required to obtain robust data on thermal alteration experienced by the shells because heated specimens may not be easily identifiable. Besides giving a one-sided perspective, the use of a single method may be affected by biases specific to the method itself, which thus can be avoided or compensated for when using two or more methods. When examining fossil shells, it is recommended to perform as many screening tests as possible to check fossil shell preservation, and this is also a valid rule in archeological settings. Only a combined application of different techniques can help to select suitable shells for isotope analysis, and also to provide deeper insights into the human past.

Acknowledgments. We thank the Ministry of Heritage and Tourism of Oman for the opportunity to investigate the site and related materials, and the Museum of Frankincense Land in Salalah for support in the field and in the study of the materials. We acknowledge L. Angiolini for comments on a first draft of the manuscript. We thank S. Crespi for technical support in the SEM acquisition of the images and C. Malinverno and M. Pegoraro for technical support in the specimen preparation. E. Ferrari is acknowledged for technical support with the stable isotope analyses. C. Corbetta is thanked for the photographs of the specimens here illustrated. The Associate Editor and two anonymous reviewers are deeply thanked for their comments and suggestions which improved the quality of the manuscript.

REFERENCES

Aldeias, V., Dibble, H.L., Sandgathe, D., Goldberg, P., McPherron, S.J.P., 2016. How heat alters underlying deposits and implications for archaeological fire features: a controlled experiment. *Journal of Archaeological Science* **67**, 64–79.

Aldeias, V., Gur-Arieh, S., Maria, R., Monteiro, P., Cura, P., 2019. Shell we cook it? An experimental approach to the microarchaeological record of shellfish roasting. *Archaeological and Anthropological Sciences* **11**, 389–407.

Almagro, Í., Drzymała, P., Rodríguez-Navarro, A.B., Sainz-Díaz, C.I., Willinger, M.G., Bonarski, J., Checa A.G., 2015. Crystallography and textural aspects of crossed lamellar layers in Arcidae (Bivalvia, Mollusca) shells. *Key Engineering Materials* **672**, 60–70.

https://doi.org/10.1017/qua.2022.62 Published online by Cambridge University Press

Andrus, C.F.T., 2011. Shell midden sclerochronology. *Quaternary Science Reviews* **30**, 2892–2905.

Andrus, C.F.T., Crowe D.E., 2002. Alteration of otolith aragonite: effects of prehistoric cooking methods on otolith chemistry. *Journal of Archaeological Science* **29**, 291–299.

Brand, U., Bitner, M.A., Logan, A., Azmy, K., Crippa, G., Angiolini, L., Colin, P., Griesshaber, E., Harper, E.M., Taddei Ruggiero, E., Häussermann, V., 2019. Brachiopod-based oxygen-isotope thermometer: update and review. *Rivista Italiana di Paleontologia e Stratigrafia* **125**, 775–787.

Brand, U., Logan, A., Bitner, M.A., Griesshaber, E., Azmy, K., Buhl, D., 2011. What is the ideal proxy of Palaeozoic seawater chemistry? *Memoirs of the Association of Australasian Palaeontologists* **41**, 9–24.

Burchell, M., Cannon, A., Hallmann, N., Schwarcz, H.P., Schöne, B.R., 2013. Refining estimates for the season of shellfish collection on the Pacific Northwest coast: applying high-resolution stable oxygen isotope analysis and sclerochronology. *Archaeometry* **55**, 258–276.

Butler, P.G., Freitas, P.S., Burchell, M., Chauvaud, L., 2019. Archaeology and sclerochronology of marine bivalves. In: Smaal, A., Ferreira, J.G., Grant, J., Petersen, J.K., Strand, Ø. (Eds.), *Goods and Services of Marine Bivalves*. Springer, Cham, pp. 413–444.

Campbell, G., 2017. "What do I do with all these shells?" Basic guidance for the recovery, processing and retention of archaeological marine shells. *Quaternary International* **427**, 13–20.

Carenti, G., Wilkens, B., 2008. Terrestrial fauna and marine produce in Sumhuram. In: Avanzini, A. (Ed.), *A Port in Arabia Between Rome and the Indian Ocean (3rd C.BC–5th C.AD)*: *Khor Rori Report* 2, L'Erma di Bretschneider, Roma, pp. 477–547.

Carter, J.G., 1990. *Skeletal Biomineralization: Patterns, Processes and Evolutionary Trends, Short Courses in Geology Vol. 5*. Van Nostrand Reinhold, New York, 832 pp.

Carter, J.G., Harries, P.J., Malchus, N., Sartori, A.F., Anderson, L.C., Bieler, R., Bogan, A.E., *et al.*, 2012. Treatise Online no. 48, Part N, Revised, Volume 1, Chapter 31: Illustrated glossary of the Bivalvia. *Treatise Online* **48**, https://doi.org/10.17161/to.v0i0.4322.

Carter, J.G., Sato, K., 2020. Treatise Online no. 137, Part N, Revised, Volume 1, Chapter 2A: Bivalve shell microstructure and mineralogy: Shell microstructure terminology. *Treatise Online* **137**, https://doi.org/10.17161/to.vi.14659.

Casella, L.A., Griesshaber, E., Yin, X., Ziegler, A., Mavromatis, V., Müller, D., Ritter, A.-C., *et al.*, 2017. Experimental diagenesis: insights into aragonite to calcite transformation of *Arctica islandica* shells by hydrothermal treatment. *Biogeosciences* **14**, 1461–1492.

Crippa, G., Angiolini, L., Bottini, C., Erba, E., Felletti, F., Frigerio, C., Hennissen, J.A.I., *et al.*, 2016a. Seasonality fluctuations recorded in fossil bivalves during the early Pleistocene: Implications for climate change. *Palaeogeography, Palaeoclimatology, Palaeoecology* **446**, 234–251.

Crippa, G., Ye, F., Malinverno, C., Rizzi, A., 2016b. Which is the best method to prepare invertebrate shells for SEM analysis? Testing different techniques on recent and fossil brachiopods. *Bollettino della Società Paleontologica Italiana* **55**, 111–125.

Crippa, G., Griesshaber, E., Checa, A.G., Harper, E.M., Simonet Roda, M., Schmahl, W.W., 2020. Orientation patterns of aragonitic crossed-lamellar, fibrous prismatic and myostracal microstructures of modern *Glycymeris* shells. *Journal of Structural Biology* **212**, 107653. https://doi.org/10.1016/j.jsb.2020.107653.

Eerkens, J.W., Byrd, B.F., Spero, H.J., Fritschi, A.K., 2013. Stable isotope reconstructions of shellfish harvesting seasonality in an estuarine environment: implications for Late Holocene San Francisco Bay settlement patterns. *Journal of Archaeological Science* **40**, 2014–2024.

Epstein, S., Buchsbaum, R., Lowenstam, H.A., Urey, H.C., 1953. Revised carbonate-water isotopic temperature scale. *Bulletin of Geological Society of America* **64**, 1315–1326.

Ferguson, J.E., Henderson, G.M., Fa, D.A., Finlayson, J.C., Charnley, N.R., 2011. Increased seasonality in the Western Mediterranean during the last glacial from limpet shell geochemistry. *Earth and Planetary Science Letters* **308**, 325–333.

Gillikin, D.P., Lorrain, A., Bouillon, S., Willenz, P., Dehairs, F., 2006. Stable carbon isotopic composition of *Mytilus edulis* shells: relation to metabolism, salinity, $\delta^{13}C_{DIC}$ and phytoplankton. *Organic Geochemistry* **37**, 1371–1382.

Gröcke, D.R., Gillikin, D.P., 2008. Advances in mollusc sclerochronology and sclerochemistry: tools for understanding climate and environment. *Geo-Marine Letters* **28**, 265–268.

Ingram, B.L., Conrad, M.E., Ingle, J.C., 1996. Stable isotope and salinity systematics in estuarine waters and carbonates: San Francisco Bay. *Geochimica et Cosmochimica Acta* **60**, 455–467.

Ivany, L.C., Runnegar, B., 2010. Early Permian seasonality from bivalve $\delta^{18}O$ and implications for the oxygen isotopic composition of seawater. *Geology* **38**, 1027–1030.

Jones, D.S., 1983. Sclerochronology: reading the record of the molluscan shell: Annual growth increments in the shells of bivalve molluscs record marine climatic changes and reveal surprising longevity. *American Scientist* **71**, 384–391.

Kobayashi, I., Kamiya, H., 1968. Microscopic observations on the shell structure of bivalves—part III, genus *Anadara*. *Journal of the Geological Society of Japan* **74**, 351–362. [in Japanese with English abstract]

Larsen, S.C., 2015. *Recrystallization of Biogenic Aragonite Shells from Archeological Contexts and Implications for Paleoenviromental Reconstruction*. Master's thesis, Western Washington University, Bellingham.

Lécuyer, C., 1996. Effects of heating on the geochemistry of biogenic carbonates. *Chemical Geology* **129**, 173–183.

Lécuyer, C., Reynard, B., Martineau, F., 2004. Stable isotope fractionation between mollusc shells and marine waters from Martinique Island. *Chemical Geology* **213**, 293–305.

Li, H., Jin, D., Li, R., Li, X., 2015. Structural and mechanical characterization of thermally treated conch shells. *JOM* **67**, 720–725.

Lindauer, S., Santos, G.M., Steinhof, A., Yousif, E., Phillips, C., Jasim, S.A., Uerpmann, H.P., Hinderer, M., 2017. The local marine reservoir effect at Kalba (UAE) between the Neolithic and Bronze Age: an indicator of sea level and climate changes. *Quaternary Geochronology* **42**, 105–116.

Lindauer, S., Milano, S., Steinhof, A., Hinderer, M., 2018. Heating mollusc shells—A radiocarbon and microstructure perspective from archaeological shells recovered from Kalba, Sharjah Emirate, UAE. *Journal of Archaeological Science: Reports* **21**, 528–537.

Lischi, S., 2018. Macroscopic analysis of the bead assemblage from the South Arabian port of Sumhuram, Oman (seasons 2000–2013). *Arabian Archaeology and Epigraphy* **29**, 65–92.

Lischi, S., 2019a. Risultati preliminari delle ricerche archeologiche presso l'insediamento HAS1 di Inqitat, Dhofar (2016–2019). *Egitto e Vicino Oriente* **42**, 119–134. [in Italian with English abstract]

Lischi, S., 2019b. Dal Paleolitico al Periodo Islamico: la storia del Dhofar attraverso lo studio archeologico dell'Inqitat/From the Paleolithic to the Islamic Period: the History of Dhofar through the archaeological study of Inqitat. In: Frenez, D., Cattani, M. (Eds.), *Sognatori/Dreamers. 40 Anni di Ricerche Archeologiche Italiane in Oman/40 Years of Italian Archaeological Research in Oman*. BraDypUS, Communicating Cultural Heritage, Roma, pp. 149–151.

Lischi, S., 2020. Beads and pendants from Inqitat (Dhofar, Sultanate of Oman). *Polish Archaeology in the Mediterranean* **29**, 337–354.

Lischi, S., 2021. Notes on the South Arabian occupation of Inqitat. In: Hatke, G., Ruzicka, R. (Eds.), *South Arabian Long-Distance Trade in Antiquity: "Out of Arabia."* Cambridge Scholars Publishing, Newcastle upon Tyne, pp. 228–244.

Mannino, M.A., Spiro, B.F., Thomas, K.D., 2003. Sampling shells for seasonality: oxygen isotope analysis on shell carbonates of the inter-tidal gastropod *Monodonta lineata* (da Costa) from populations across its modern range and from a Mesolithic site in southern Britain. *Journal of Archaeological Science* **30**, 667–679.

Mannino, M.A., Thomas, K.D., Leng, M.J., Piperno, M., Tusa, S., Tagliacozzo, A., 2007. Marine resources in the Mesolithic and Neolithic at the Grotta dell'Uzzo (Sicily): evidence from isotope analyses of marine shells. *Archaeometry* **49**, 117–133.

Mannino, M.A., Thomas, K.D., Leng, M.J., Di Salvo, R., Richards, M.P., 2011. Stuck to the shore? Investigating prehistoric hunter-gatherer subsistence, mobility and territoriality in a Mediterranean coastal landscape through isotope analyses on marine mollusc shell carbonates and human bone collagen. *Quaternary International* **244**, 88–104.

https://doi.org/10.1017/qua.2022.62 Published online by Cambridge University Press

McConnaughey, T.A., Gillikin, D.P., 2008. Carbon isotopes in mollusk shell carbonates. *Geo-Marine Letters* **28**, 287–299.

Milano, S., Nehrke, G., 2018. Microstructures in relation to temperature-induced aragonite-to-calcite transformation in the marine gastropod *Phorcus turbinatus*. *PLoS ONE* **13**, e0204577. https://doi.org/10.1371/journal.pone.0204577.

Milano, S., Prendergast, A.L., Schöne, B.R., 2016. Effects of cooking on mollusk shell structure and chemistry: Implications for archaeology and paleoenvironmental reconstruction. *Journal of Archaeological Science: Reports* **7**, 14–26.

Milano, S., Lindauer, S., Prendergast, A.L., Hill, E.A., Hunt, C.O., Barker, G., Schone, B.R., 2018. Mollusk carbonate thermal behaviour and its implications in understanding prehistoric fire events in shell middens. *Journal of Archaeological Science: Reports* **20**, 443–457.

Moon, L.R., Judd, E.J., Thomas, J., Ivany, L.C., 2021. Out of the oven and into the fire: Unexpected preservation of the seasonal $\delta^{18}O$ cycle following heating experiments on shell carbonate. *Palaeogeography, Palaeoclimatology, Palaeoecology* **562**, 110115. https://doi.org/10.1016/j.palaeo.2020.110115.

Morandi Bonacossi, D., 2004. Coloni hadramiti e popolamento indigeno nel Paese dell'Incenso (Dhofar, Sultanato dell'Oman) fra V sec. a.C. e VI secolo d.C. Una sintesi preliminare. In: Fales, F.M, Morandi, Morandi Bonacossi, D. (Eds.), *Mesopotamia e Arabia. Scavi Archeologici e Studi Territoriali delle Università Trivenete (1994–1998)*, Istituto Veneto di Scienze, Lettere ed Arti, Venezia, pp. 179–216. [in Italian]

Müller, P., Staudigel, P.T., Murray, S.T., Vernet, R., Barusseau, J-P., Westphal, H., Swart, P.K., 2017. Prehistoric cooking versus accurate paleotemperature records in shell midden constituents. *Scientific Reports* **7**, 3555. https://doi.org/10.1038/s41598-017-03715-8.

Newton, L.S., Zarins, J., 2019. *Dhofar through the Ages: An Ecological, Archaeological and Historical Landscape. The Archaeological Heritage of Oman 1*. Archaeopress Publishing Ltd., Oxford, 128 pp.

Nouet, J., Chevallard, C., Farre, B., Nehrke, G., Campmas, E., Stoetzel, E., El Hajraoui, M.A., Nespoulet, R., 2015. Limpet shells from the Aterian Level 8 of El Harhoura 2 Cave (Témara, Morocco): preservation state of crossed-foliated layers. *PLoS One* **10**, e0137162. https://doi.org/10.1371/journal.pone.0137162.

O'Neil, J.R., Clayton, R.N., Mayeda, T.K., 1969. Oxygen isotope fractionation in divalent metal carbonates. *Journal of Chemical Physics* **51**, 5547–5558.

Oschmann, W., 2009. Sclerochronology: editorial. *International Journal of Earth Sciences* **98**, 1–2.

Prendergast, A.L., Stevens, R.E., O'Connell, T.C., Fadlalak, A., Touati, M., Al-Mzeine, A., Schöne, B.R., Hunt, C.O., Barker, G.W., 2016. Changing patterns of eastern Mediterranean shellfish exploitation in the Late Glacial and Early Holocene: oxygen isotope evidence from gastropods in Epipaleolithic to Neolithic human occupation layers at the Haua Fteah cave, Libya. *Quaternary International* **407**, 80–93.

Richards, M.P., Jacobi, R., Cook, J., Pettitt, P.B., Stringer, C.B., 2005. Isotope evidence for the intensive use of marine foods by Late Upper Palaeolithic humans. *Journal of Human Evolution* **49**, 390–394.

Rodriguez-Navarro, A.B., Checa, A., Willinger, M-G., Bolmaro, R., Bonarski, J., 2012. Crystallographic relationships in the crossed lamellar microstructure of the shell of the gastropod *Conus marmoreus*. *Acta Biomaterialia* **8**, 830–835.

Schöne, B.R., 2008. The curse of physiology—challenges and opportunities in the interpretation of geochemical data from mollusk shells. *Geo-marine Letters* **28**, 269–285.

Schöne, B.R., 2013. *Arctica islandica* (Bivalvia): A unique paleoenvironmental archive of the northern North Atlantic Ocean. *Global and Planetary Change* **111**, 199–225.

Schöne, B.R., Surge, D.M., 2012. Treatise Online no. 46, Part N, Revised, Volume 1, Chapter 14: Bivalve sclerochronology and geochemistry. *Treatise Online* **46**. https://doi.org/10.17161/to.v0i0.4297.

Schöne, B.R., Gillikin, D.P., 2013. Unraveling environmental histories from skeletal diaries—Advances in sclerochronology. *Palaeogeography, Palaeoclimatology, Palaeoecology* **373**, 1–5.

Shackleton, N.J., 1973. Oxygen isotope analysis as a means of determining season of occupation of prehistoric midden sites. *Archaeometry* **15**, 133–141.

Staudigel, P.T., Swart, P.K., 2016. Isotopic behavior during the aragonite-calcite transition: Implications for sample preparation and proxy interpretation. *Chemical Geology* **442**, 130–138.

Staudigel, P.T., Swart, P.K., Pourmand, A., Laguer-Díaz, C.A., Pestle, W.J., 2019. Boiled or roasted? Bivalve cooking methods of early Puerto Ricans elucidated using clumped isotopes. *Science Advances* **5**, 5447–5474.

Taylor, J.D., Kennedy, W.J., Hall, A., 1969. The shell structure and mineralogy of the Bivalvia: introduction, Nuculacea–Trigonacea. *Bulletin of the British Museum of Natural History, Zoology* **3**, 1–125.

Tursch, B., Machbaete, Y., 1995. The microstructure of the shell in the genus *Oliva* (Studies on Olividae. 24). *APEX* **10**, 61–78.

Urey, H.C., 1947. The thermodynamic properties of isotopic substances. *Journal of the Chemical Society*, 562–581.

Wrangham, R., 2009. *Catching Fire: How Cooking Made Us Human*. Basic Books, New York, 320 pp.

Wrangham, R., Carmody, R., 2010. Human adaptation to the control of fire. *Evolutionary Anthropology* **19**, 187–199.

https://doi.org/10.1017/qua.2022.62 Published online by Cambridge University Press